

**Magnetic exchange effects in PbS/Fe/EuS/PbS thin films**V. V. Volobuev,<sup>1,2</sup> A. N. Stetsenko,<sup>2</sup> A. Yu. Sipatov,<sup>2</sup> and J. van Lierop<sup>1</sup><sup>1</sup>*Department of Physics and Astronomy, University of Manitoba, Winnipeg, Manitoba, Canada R3T 2N2*<sup>2</sup>*Department of Physics of Metals and Semiconductors, National Technical University "Kharkiv Polytechnical Institute," Kharkiv, Ukraine*

(Received 24 November 2009; published 23 April 2010)

The magnetism of ferromagnetic metal/ferromagnetic semiconductor PbS/EuS/Fe/PbS thin films has been studied. The presence of antiferromagnetic alignment of neighboring ferromagnetic layers in direct contact with each other was observed. The films also showed an exchange bias effect which appeared due to the formation (likely during film deposition) of antiferromagnetic FeS at the Fe/PbS interface. Antiferromagnetic interfacial exchange coupling between Fe and FeS was also observed. It was shown that the exchange anisotropy could be controlled by the remnant state of Fe magnetization during the cooling process, that in turn could be tuned by an external cooling field. The influence of exchange anisotropy and exchange coupling effects on the field and temperature dependencies of the film magnetization was examined.

DOI: [10.1103/PhysRevB.81.134430](https://doi.org/10.1103/PhysRevB.81.134430)

PACS number(s): 75.70.-i, 75.40.-s, 75.50.Pp

**I. INTRODUCTION**

The magnetism of ferromagnetic semiconductors (FS) that are in direct contact with ferromagnetic (FM) 3*d* transitional metals is of interest presently as exchange interactions at the interface between the two ferromagnetic materials can lead to some unusual and useful properties. Using a ferromagnetic semiconductor in this configuration will enable a nearly 100% spin polarization for spin injection into semiconductors,<sup>1</sup> demonstrated successfully in EuS/Co (Ref. 2) and EuS/Gd (Ref. 3) systems. Promising results were also obtained in a Fe/GaMnAs system.<sup>4</sup> EuS is well-known Heisenberg ferromagnetic semiconductor [ $E_g=1.65$  eV,  $T_C=16.5$  K (Ref. 5)] which has a negligible free carrier concentration. Also, EuS's very large conduction band splitting of 0.36 eV (Ref. 6) makes it a contender for utilization in semiconductor spintronics.

Together with enhanced spin-filtering properties, FS/FM systems are believed to exhibit a magnetic proximity effect,<sup>7</sup> where interfacial moments of the FS order at temperatures significantly above the FS's intrinsic magnetic ordering temperature ( $T_C$ ) via coupling with the FM with a higher  $T_C$ .<sup>8-10</sup> Increasing the  $T_C$  of the FS to room temperature would make such systems useful for spintronic applications. An enhanced EuS  $T_C$  from a magnetic proximity effect was reported in a EuS/Co multilayer<sup>11</sup> and nanocomposite (EuS precipitate particles in Co matrix).<sup>12</sup>

Another interesting phenomenon that has been observed in FS/FM multilayer structures is exchange coupling.<sup>13</sup> This effect was observed in EuS/Co,<sup>11,14,15</sup> EuS/Fe,<sup>16</sup> Fe/GaMnAs (Ref. 7) multilayers, and EuS/Co nanocomposites.<sup>12,17</sup> In all these cases antiferromagnetic (AF) coupling, where magnetic moments of neighboring ferromagnetic layers are in opposite directions, have been reported.

In this paper we present results obtained on EuS/Fe-based thin films. Most of the previous work has been performed on EuS/Co systems. Fe with a  $\sim 30\%$  larger free ion moment than Co and a lower bulk  $T_C$  ( $T_C=1043$  K in bulk Fe and 1388 K in bulk Co) should provide different proximity-based nanomagnetism, e.g., enhanced  $T_C$ 's and exchange coupling.

The structure and magnetism of PbS/EuS/Fe/PbS thin films have been investigated, where antiferromagnetic exchange coupling between Fe and EuS has been observed. However, unlike EuS/Co-based films, we did not detect a proximity effect enhanced  $T_C$  for the EuS FS.

**II. EXPERIMENTAL METHODS**

Thin films were prepared with a PbS/EuS ( $t$  nm)/Fe ( $t$  nm)/PbS, where  $t=5-20$  nm, configuration. Since all the samples (with different layer thickness) showed similar magnetic behavior, in this paper we will focus on the PbS/EuS (10 nm)/Fe (10 nm)/PbS composition. The films were deposited in high vacuum ( $10^{-7}-10^{-8}$  Torr) onto a (001) KCl substrate using electron-beam evaporation of Fe and EuS, and thermal evaporation of PbS from a tungsten boat. The KCl substrate was cleaved in air and placed immediately into the vacuum chamber. Film thickness and growth rates were controlled using a calibrated quartz balance resonator. The deposition rate for all the films components was 0.05–0.2 nm/s. All films had a 20 nm PbS capping layer to prevent possible film oxidation and a PbS buffer layer of the same thickness that permitted epitaxial growth of EuS. Epitaxial EuS/PbS multilayers on (001) KCl with well-defined interfaces and layer thicknesses down to several monolayers can be manufactured with the KCl substrate at 250 °C.<sup>18</sup> To ensure a continuous and smooth interface between the EuS and Fe layers, and prevent any possible intermixing, a two stage process was used during film growth. An epitaxial EuS layer on a buffer PbS layer was first deposited at 270 °C, the substrate was cooled to room temperature, and then the Fe and capping PbS layers were deposited.

To investigate the film layer microstructures with transmission electron microscopy (TEM), the KCl substrate was dissolved in distilled water and the film placed onto TEM grids. Magnetic measurements were performed with a commercial Quantum Design MPMS-XL magnetometer/susceptometer. External magnetic fields were applied parallel to the sample's plane in the [100] direction of EuS. Before taking measurements, either field cooling (FC) or zero-field

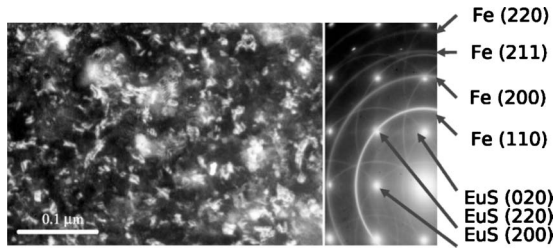


FIG. 1. Plane view transmission electron microscope image of a PbS (20 nm)/EuS (10 nm)/Fe(10 nm) film (left) and its electron-diffraction pattern (right).

cooling (ZFC), sometimes combined with demagnetization using minor loop procedures, was performed.

### III. RESULTS AND DISCUSSION

A representative TEM image and electron diffraction pattern of the PbS (20 nm)/EuS (10 nm)/Fe (10 nm) film is shown in Fig. 1. The grains shown in the TEM image and rings of the electron-diffraction pattern correspond to continuous polycrystalline Fe. The lattice constant of Fe was  $2.90 \pm 0.04$  Å, in good agreement with the bulk value.<sup>19</sup> The EuS and PbS show electron-diffraction patterns of a (001) monocrystalline thin film. The spots from these materials could not be resolved, indicating that monocrystalline EuS had grown onto the PbS pseudomorphically (with the same in-plane lattice constant  $a=5.94 \pm 0.12$  Å), which was also in good agreement with the bulk value of PbS  $a=5.9362$  Å.<sup>20</sup> The observed pseudomorphic growth indicated a van der Merve growth mechanism in a layer-by-layer fashion. X-ray and neutron-diffraction experiments performed on EuS-PbS superlattices grown in a similar fashion showed satellites near Bragg peaks and at grazing angles demonstrating that high-quality samples could be obtained with layer thickness of one monolayer.<sup>21</sup> From these results we estimated that the PbS/EuS interface roughness was on the order of a single EuS monolayer ( $\sim 0.3$  nm). Due to the layer-by-layer growth of the EuS, the top of the film surface (e.g., an interface) should be smooth. Smooth interfaces between EuS and Fe with no intermixing have been reported previously.<sup>16,22</sup> The level of roughness and possible intermixing of phases expected at the EuS/Fe interface roughness should have been on the order of a couple Fe lattice constants. Furthermore, an electron microscopy study revealed an Fe layer without texture and an average grain size of  $\sim 3$  nm. Since it was unlikely that the interface roughness was larger than the average grain size of the constituent materials, we propose a maximum roughness of the Fe/PbS interface of  $\sim 3$  nm. We did not find any evidence of additional phases in the PbS/Fe/EuS/PbS film samples (except rings from the polycrystalline PbS top layer in the electron-diffraction patterns). As the TEM could not resolve crystallites or layers less than 1 nm in thicknesses, if additional phases were present, they could not exceed 1 nm in thickness providing an upper bound on the degree (thickness) of possible intermixing.

The temperature dependence of the ac susceptibility in Fig. 2 showed a sharp peak in the in-phase ( $\chi'$ ) component at

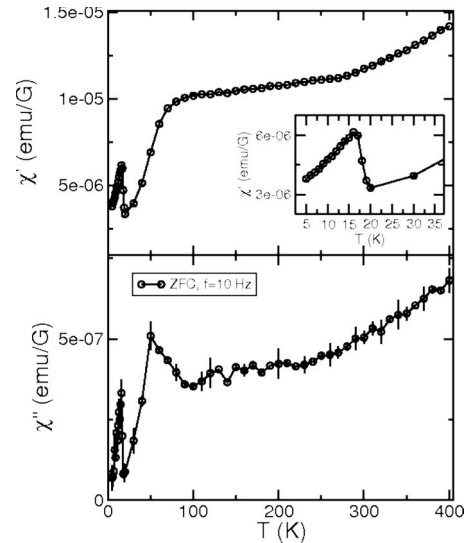


FIG. 2. In-phase ( $\chi'$ ) and out-of-phase ( $\chi''$ ) temperature dependence of the ac susceptibility of the PbS (20 nm)/EuS (10 nm)/Fe (10 nm)/PbS (20 nm) film using a 1 Oe drive field oscillating at 10 Hz. The inset shows  $\chi'(T)$  for temperatures around the EuS  $T_C$ .

16.5 K, and similar behavior in the out-of-phase component at a slightly lower temperature indicating the onset of hysteresis (with cooling). Both features correspond to the Curie temperature,  $T_C$ , of the EuS film component. The frequency independence of this feature (from 10 to 1 kHz, not shown) was consistent with a magnetic ordering process. While the  $T_C$  of EuS thin films could be altered by thickness (finite-size) effects and strain, e.g., film-substrate lattice mismatch and thermal-expansion differences between film substrate, our measured  $T_C$  was in excellent agreement with 10 nm thick EuS on KCl.<sup>18</sup> At intermediate temperatures (above the EuS  $T_C$ ) a further increase in  $\chi_{ac}(T)$  with warming was observed (Fig. 2) that did exhibit a measuring frequency dependence, magnetism consistent with “unblocking” of single-domain-sized crystallites.<sup>9,10</sup> Above 100 K, this frequency dependence collapsed, and with warming a slow increase in  $\chi_{ac}(T)$  indicated the presence of superparamagnetism. The change in  $\chi_{ac}(T)$ 's slope between  $\sim 100$  and 300 K, and from 300 to 400 K suggested that there may have been a magnetic phase that was undetectable in the microstructure and composition studies described above. A likely candidate would be FeS at the Fe/PbS interface which would alter the magnetism significantly.

Magnetic hysteresis loops of the EuS/Fe film at 2.5 K were measured after cooling from 400 K in different magnetic fields with the results presented in Fig. 3. The loops were shifted along the field direction, similar in nature to loops of exchange bias systems.<sup>8–10,23</sup> The origin of this loop shift could be the presence of an AF or ferrimagnetic layer near the FM or FS interfaces. To examine this possibility, films of 10 nm single layers of Fe or EuS, sandwiched between two 20 nm layers of PbS using the procedure described above, were prepared. The EuS film exhibited typical ferromagnetic behavior with  $T_C \sim 16.5$  K and no observable loop shift. However, the Fe film showed a negative loop shift along the field direction (Fig. 4), further evidence of a small

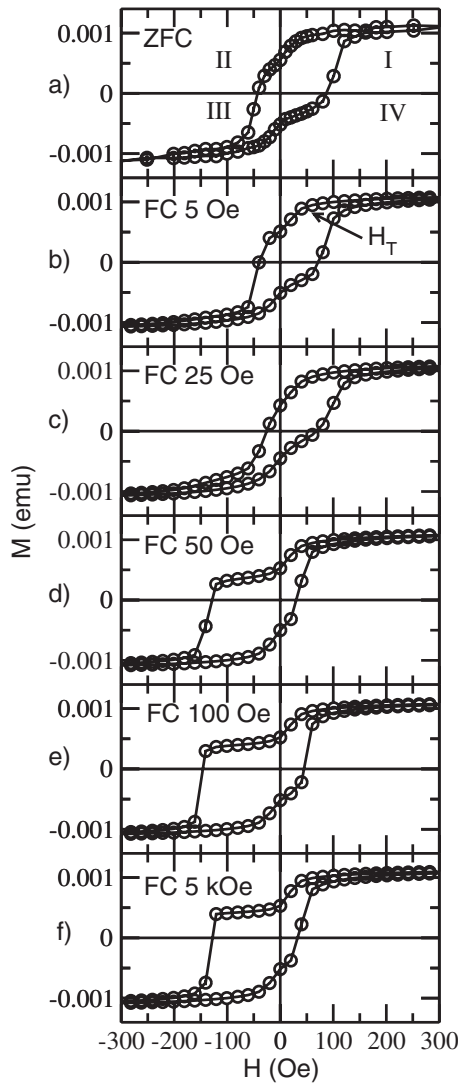


FIG. 3. Hysteresis loops ( $\pm 20$  kOe) of the PbS (20 nm)/EuS (10 nm)/Fe (10 nm)/PbS (20 nm) film at 2.5 K measured after (a) ZFC, (b) 5 Oe FC, (c) 25 Oe FC, (d) 50 Oe FC, (e) 100 Oe FC, and (f) 5000 Oe FC. Cooling was performed from 400 K in all cases. The lines are guides to the eye. I-II-III-IV is the order of the loop cycle.  $H_T$  corresponds to the field where a change from parallel to antiparallel alignment between EuS and Fe magnetization occurs.

amount of FeS at the Fe/PbS interface that was suggested by the intermediate temperature  $\chi_{ac}(T)$  behavior (above). A very thin FeS layer at the Fe/PbS interface left (unresolvable dur-

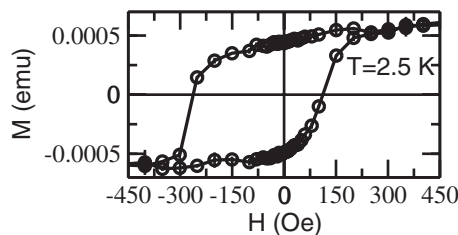


FIG. 4. Hysteresis loop ( $\pm 20$  kOe) of the PbS (20 nm)/Fe (10 nm)/PbS (20 nm) film at 2.5 K measured after ZFC from 400 K. The lines are guides to the eye.

ing the TEM investigations) arose likely during thin film fabrication from a reduction in PbS by the Fe. Comparing the Gibbs free energy changes in the constituents ( $\Delta G$ ) using data from Ref. 24, the reaction  $\text{PbS} + \text{Fe} \rightarrow \text{FeS} + \text{Pb}$  is thermodynamically favorable, even at room temperature, given the energy gain  $\Delta G_{298}^\circ = -5.28$  kJ/mol. In Ref. 25 this reaction has been studied in detail at the nanoscale and observed at room temperature. FeS with a structure of NiAs is an AF with Néel temperature ( $T_N$ ) around 600 K.<sup>26</sup> A spin transition can occur around 445 K that involves Fe spins rotating from a parallel to a perpendicular-to-the-hexagonal axis direction.<sup>27</sup> In addition, FeS displays ferrimagnetic properties when it is Fe deficient.<sup>26</sup>

An exchange bias blocking temperature [where  $H_{ex}(T) = 0$ ] of  $T_B \sim 20$  K was observed, in agreement with the  $T_B$  indicated by the  $\chi_{ac}(T)$  results (Fig. 2) that showed evidence of the FeS crystallites (presumably of similar area as the Fe crystallites but around a monolayer in thickness) unblocking. With the FeS crystallites superparamagnetic, the  $T_B$  of the two processes (superparamagnetic and exchange bias) would coincide. While  $T_N \sim 600$  K for FeS and  $T_B \ll T_N$  is usual, a similar difference in  $T_B$  and  $T_N$  has been observed recently in Fe/FeO thin films with an ultrathin iron-oxide layer.<sup>28</sup> It is likely that the significant differences between the ordering and exchange coupling energies is an indication of the weak coupling between the FeS and EuS components [likely due of the sparseness of the FeS (AF) layer].<sup>29</sup>

It should be noted that  $H_{ex}$  due to exchange coupling between the Fe and (possible) FeS interfacial moments occurred even when the film was zero-field cooled (i.e., no external field was present to set the interfacial moment configurations to permit a unidirectional anisotropy, a typical prerequisite for exchange bias<sup>29</sup>), shown in Fig. 3. However, a proximity-enhanced “local” ordering of the interfacial moments may be occurring, analogous to that observed recently in AF/FM thin films.<sup>8,9</sup>

An enhancement of the coercivity  $H_c$  of an exchange biased system compared to that of the bare FM is typical.<sup>29</sup>  $H_c$  of the PbS/Fe/PbS film was nearly twice that of the PbS/EuS/Fe/PbS film at the same temperature. This difference in  $H_c$ 's was likely due to the presence of two FeS interlayers in PbS/Fe/PbS sample, resulting in a further enhancement coupling. In addition, heating a PbS/Fe/PbS film to  $\sim 300$  °C in an argon atmosphere led a to further increase in  $H_c$ , and a significant reduction in the net magnetization, consistent with the further reduction in PbS by Fe (e.g., a thicker AF FeS layer).

The  $M$ - $H$  loop shape of the PbS/EuS/Fe/PbS multilayer was indicative of spin valve behavior (Fig. 3). The steplike features in the hysteresis loops were the result of exchange coupling between EuS and Fe, as observed previously.<sup>16</sup> Also, the measured cooling field dependence was in agreement with previous work that had shown the amount and direction of the loop shift in AF/FM structures depended upon the amount and direction of remnant magnetization at  $T_B$  of the FM which, in turn, could be tuned by the applied cooling field.<sup>30-32</sup> This trend was observed in the PbS/EuS/Fe/PbS system [Figs. 3(a)–3(d)]. Also, for the EuS/Fe based system, due to the presence of FeS at the EuS/Fe interface, the  $M$ - $H$  behavior of the PbS/EuS/Fe/PbS multilayer was



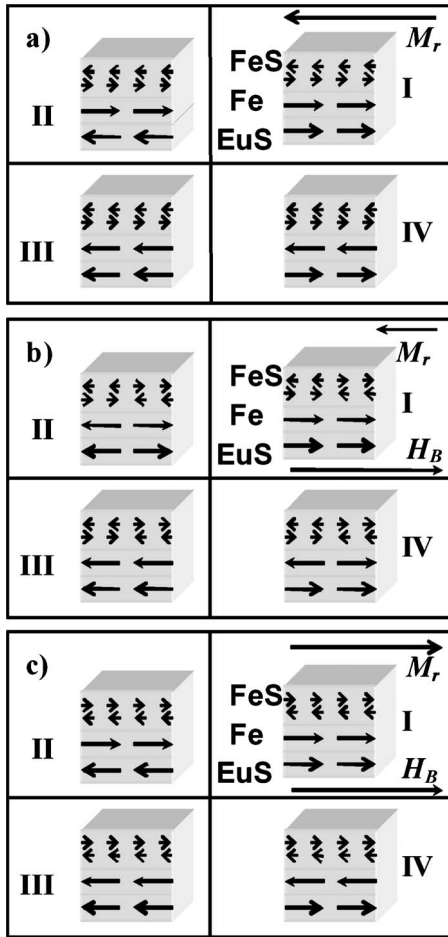


FIG. 5. Scheme of the magnetic configuration in the PbS (20 nm)/EuS (10 nm)/Fe (10 nm)/PbS (20 nm) film at 2.5 K which is correspondent to hysteresis loops presented in (a) Fig. 3(a), (b) Figs. 3(b) and 3(c), (c) Figs. 3(d) and 3(e).  $M_r$  and  $H_B$  show direction of Fe remnant magnetization and magnetic field, respectively, during the cooling through  $T_B$ .

due to the combined magnetizations and domain rotations of the Fe moments in the applied magnetic field ( $H$ ) pinned by FeS, with moments of the magnetically soft EuS layer able rotate more freely with changes in  $H$ . Furthermore, the observed “steps” in the hysteresis loops are evidence that the EuS and Fe magnetizations were aligned in opposite directions.

A schematic representation of the spin configurations that resulted in the  $M$ - $H$  loop behavior shown in Fig. 3 is presented in Fig. 5. First, consider the loop presented in Fig. 3(a) that was obtained by a ZFC process from 400 to 2.5 K (through  $T_B$ ) after a negative field at 400 K was used to saturate the FM component. The corresponding schematic image of the magnetic configuration is presented in Fig. 5(a). During the cooling through  $T_B$ , interfacial magnetic moments of the AF (FeS) were set in a configuration provided by the remnant magnetization ( $M_r$ ) of the FM (Fe). Starting the  $M$ - $H$  loop measurement from +20 kOe (quarter I of the loop cycle) Fe and EuS were magnetized to saturation in a direction opposite to  $M_r$ . The reduction in the magnetic field during the loop measurement to  $H_T \approx 50$  Oe led to rotation of

the EuS moments in a direction opposite to the Fe moments due to AF exchange coupling between the Fe and EuS.<sup>16</sup> With the applied field changing from positive to negative, a small step in the hysteresis loop was measured [Fig. 3(a)] whose presence was due to the Fe/EuS coupling facilitating an antiparallel orientation of Fe and EuS moments (i.e., the Zeeman and anisotropy energy terms were weaker) as shown schematically in quarter II of the loop cycle of Fig. 5(a). A further increase in the negative field made Fe moments rotate into the field direction [quarter III of the loop cycle in Fig. 5(a)]. The  $M$ - $H$  behavior going from positive to negative fields was analogous to what the film experienced during a field scan from positive to negative  $H$  [quarter IV of the loop cycle, Fig. 5(a)], except that in large positive fields the film was magnetized along the “hard axis” set by the exchange and unidirectional anisotropy which created a energy barrier which needed to be overcome before Fe moments could align with  $H$ . This competition resulted in the observed step in the IV quarter of the loop over a larger field range than the step obtained for positive-to-negative field change. Cooling the film in 5 or 25 Oe [Figs. 3(b) and 3(c)] permitted some Fe domains to change their orientation, which decreased the total  $M_r$ . This in turn resulted in an effective weakening of the unidirectional anisotropy of Fe moments at the interface, and thus a decrease in  $H_{ex}$ ,  $H_c$ , and reduction in the step’s length [Fig. 5(b)]. A further increase in the cooling field to 50 or 100 Oe [Figs. 3(d) and 3(e)] set the majority of Fe domain moments in the direction of the field [Fig. 5(c)] so that the loops shift in a negative field direction. Increasing the cooling field to +5000 Oe [Fig. 3(f)] reduced the  $H_{ex}$  and  $H_c$ , likely due to FeS interfacial moments coupled antiferromagnetically to Fe moments, with the cooling field large enough to permit them to rotate into field direction.<sup>33,34</sup>

Following the 5 kOe FC  $M$ - $H$  loop, the film was warmed to 400 K and the magnetization set in its positive remnant (+ $M_r$ ) state. The film was then cooled in a negative fields of -5 Oe, -100 Oe, and -5 kOe shown in Figs. 6(a)–6(c), respectively. The loop results for the negative FC procedure were essentially the same as the positive FC ones presented in Fig. 3, except that the loops were shifted in the opposite field direction. Demagnetizing the EuS/Fe film using minor loops cycles ( $M_r \sim 10^{-6}$  emu at 300 K) followed by a ZFC procedure resulted in the loop shown in Fig. 6(d). Due to a very small unidirectional anisotropy with a concomitant reduction in the Fe coercivity,  $H_{ex} \sim -5$  Oe, resulting in no steplike features in quadrants II and IV of the  $M$ - $H$  loop, behavior that is consistent with our description above.

An inelaborate description can be constructed considering an applied field  $H_T$ , shown in Fig. 3(b), that corresponds to the field required to shift the interfacial magnetizations of Fe and EuS from parallel to antiparallel alignment. The exchange coupling energy should be equal to the Zeeman (magnetic field) energy. That is,  $\vec{H}\vec{M}_{Fe}t_{Fe} + \vec{H}\vec{M}_{EuS}t_{EuS} = -J\vec{M}_{Fe}\vec{M}_{EuS}/|\vec{M}_{Fe}||\vec{M}_{EuS}|$ , where  $\vec{H}$  is the applied field,  $\vec{M}$  the magnetization of the EuS or Fe components,  $t$  the film component thickness, and  $J$  the exchange coupling constant. For 2.5 and 5 K (well below the EuS  $T_C$ ) we found  $J_{Fe/EuS} \sim 0.15$  erg/cm<sup>2</sup> which is in good agreement with previous reports of  $J_{Fe/EuS} = 0.2$  erg/cm<sup>2</sup> (Ref. 16) and  $J_{Co/EuS}$

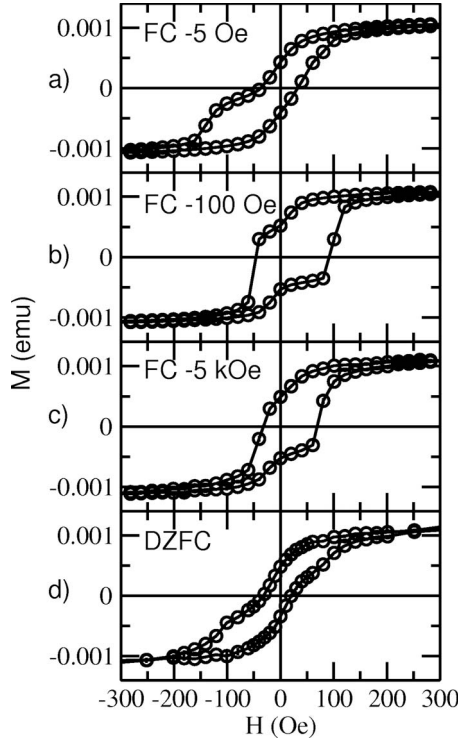


FIG. 6. Hysteresis loops ( $\pm 20$  kOe) of the PbS (20 nm)/EuS (10 nm)/Fe (10 nm)/PbS (20 nm) film at 2.5 K measured after (a)  $-5$  Oe FC, (b)  $-100$  Oe FC, (c)  $-5000$  Oe FC, and (d) after demagnetizing procedure and ZFC. Cooling was performed from 400 K in all cases. The lines are guides to the eye.

$=0.1$  erg/cm<sup>2</sup> (Ref. 15). A rough estimate of the exchange anisotropy energy at the Fe/FeS interface can be calculated<sup>29</sup> using  $\Delta E_{\text{Fe/FeS}} = H_{\text{ex}} M_{\text{Fe}} J_{\text{Fe}}$ . The maximum value of exchange anisotropy energy obtained for 2.5 K and cooling field of 100 Oe [Fig. 3(e)] is  $\Delta E_{\text{Fe/FeS}} = 0.085$  erg/cm<sup>2</sup>.

The temperature dependencies of  $H_{\text{ex}}$  and  $H_c$ , presented in Fig. 7 for the different FC procedures, revealed further information about the magnetism of the unidirectional anisotropy. For example, when the film was demagnetized and ZFC,  $H_{\text{ex}}(T)$  was essentially zero, consistent with a very small amount of interfacial FeS moments exchange coupled to the Fe moments during cooling that provided the unidirectional anisotropy. However, when the cooling field was large enough to set  $H_{\text{ex}}$ , irrespective of the cooling field strength,  $|H_{\text{ex}}(T)|$  was essentially unchanged. By contrast, for  $H_c(T)$ , starting from 2.5 K for the demagnetized ZFC, ZFC, and negative FC conditions,  $H_c(T)$  increased with warming until 15 K. However, for positive FC,  $H_c(T)$  decreased constantly. It would seem that both domain-wall (incoherent) and rotational (coherent) reversal processes in the film system are affected by the initial magnetic configuration of the film, essentially set by the field-cooling procedure. After 15 K  $H_c(T)$  rapidly decreases with warming until 50 K, as the thermal energy gradually overwhelms the anisotropy energies.

A further indication of the antiferromagnetic nature of the exchange coupling between the Fe and EuS was provided by the temperature dependencies of the low-field magnetization (Fig. 8). First, the sample was magnetized with a positive

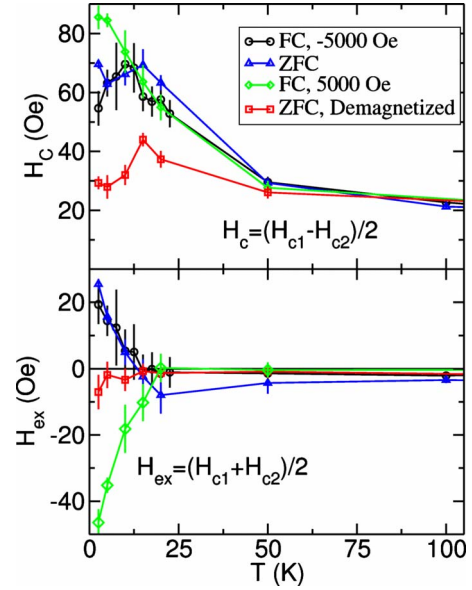


FIG. 7. (Color online) Temperature dependence of the coercivity,  $H_c = (H_{c1} + H_{c2})/2$ , and field shift,  $H_{\text{ex}} = (H_{c1} - H_{c2})/2$ , of the EuS/Fe film when  $-5000$  Oe FC ( $\circ$ ), ZFC ( $\triangle$ ),  $+5000$  Oe FC ( $\diamond$ ), and thermally demagnetized before ZFC ( $\square$ ).

field and then ZFC from 50 K (well above  $T_B$ ) in its remnant magnetization state and warmed up in a zero field to 50 K. After that the sample was again ZFC and 5 Oe was applied during its heating to 50 K. This procedure was repeated for each new magnetic field so that during cooling, the film stayed in a remnant state from the application of the magnetic field from the previous procedure. A strong reduction in the magnetization below the EuS  $T_C$  was observed when the film was warmed up in 0, 5, and 20 Oe, and this behavior is connected to the opposite alignment of EuS and Fe moments at and around the interface. With an increase in temperature from 5 to 16.5 K (EuS  $T_C$ ), there was a gradual increase in the measured magnetization as the EuS's magnetization and coupling between the Fe-EuS moments decreased with warming, until it was constant as only the Fe magnetization

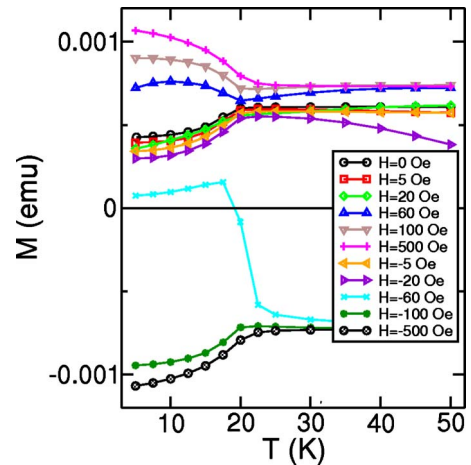


FIG. 8. (Color online) Temperature dependence of low-field magnetization obtained for PbS (20 nm)/EuS (10 nm)/Fe (10 nm)/PbS (20 nm) film using ZFC.

was present at the higher temperatures. The application of a magnetic field that was larger or equal to 60 Oe led to a rearrangement of the EuS and Fe interfacial moments with EuS and Fe moments now aligned in the same direction because the energy gained from the field (Zeeman energy) was larger than the energy associated with the AF coupling at the EuS/Fe interface. In 60 Oe, below 10 K, the measured magnetization decreased due to competition between the Fe-EuS exchange and EuS magnetic moments rotating in a direction opposite to the Fe moment direction set by the applied magnetic field. Applying a small negative magnetic field, e.g.,  $-5$  Oe, provided too small a Zeeman energy to reverse the majority of Fe moment in their domains, therefore the magnetization's temperature dependence was essentially the same as for the 0, 5, and 20 Oe cases. Of interest are the features obtained in the  $-20$  and  $-60$  Oe magnetization measurements. At temperatures below 20 K the film demonstrated similar behavior as that observed during the 0, 5, 20, and  $-5$  Oe field measurements, i.e., behavior connected to the antialignment of Fe and EuS moments. However, above 20 K when the exchange anisotropy disappeared and  $H_c$  decreased (Fig. 7), the Fe moments began to rotate into the applied field direction. Using a  $-60$  Oe field above 20 K was enough to align the Fe moments in the negative field direction. Application of larger fields, e.g.,  $-100$  and  $-500$  Oe, forced magnetic moments of the Fe and EuS to align into the negative field direction at all temperatures below 20 K, therefore providing a "mirror image" of the magnetization's temperature dependence measured in 100 and 500 Oe fields.

The observed antiferromagnetic coupling between Fe and EuS can be understood intuitively through a comparison with

the well-known behavior of Gd that couples antiferromagnetically to the transition metals in thin film form.<sup>13</sup> That is,  $\text{Eu}^{2+}$  ions in EuS have the angular momentum as Gd with  $S=J=7/2$ .<sup>5</sup> The coupling mechanism between the rare-earth and  $3d$  transition metals in multilayers is thought to be through indirect  $3d-5d-4f$  interactions, and analogous to coupling in magnetic alloys. Since Fe is at the opposite end of the  $d$ -transition series from rare earths, it is expected that their moments couple antiferromagnetically,<sup>35</sup> which is the behavior observed in the EuS/Fe based film system.

In conclusion, we have investigated the structural and magnetic properties of PbS/EuS/Fe/PbS thin films. It was shown that FeS was likely formed at the Fe/PbS interface during thin film deposition and was the origin of the measured unidirectional exchange anisotropy. The magnitude of the exchange anisotropy depended on the Fe remnant magnetization during the cooling procedure and could be tuned by cooling field. The maximum value of exchange anisotropy energy was found to be  $0.085$  erg/cm<sup>2</sup> at 2.5 K. Antiferromagnetic exchange coupling between the Fe and EuS net magnetic moments was also observed in this system. The value of Fe/EuS exchange coupling constant was estimated to be  $0.15$  erg/cm<sup>2</sup> at 2.5 K.

#### ACKNOWLEDGMENTS

This work was supported by grants from the Natural Sciences and Engineering Research Council of Canada and the Canada Foundation for Innovation.

- 
- <sup>1</sup>G. Schmidt, *J. Phys. D* **38**, 107 (2005).  
<sup>2</sup>T. Nagahama, T. S. Santos, and J. S. Moodera, *Phys. Rev. Lett.* **99**, 016602 (2007).  
<sup>3</sup>C. J. P. Smits, A. T. Filip, J. T. Kohlhepp, H. J. M. Swagten, B. Koopmans, and W. J. M. D. Jonge, *J. Appl. Phys.* **95**, 7405 (2004).  
<sup>4</sup>S. Mark, C. Gould, K. Pappert, J. Wenisch, K. Brunner, G. Schmidt, and L. W. Molenkamp, *Phys. Rev. Lett.* **103**, 017204 (2009).  
<sup>5</sup>P. Wachter, in *Hanbook on the Physics and Chemistry of Rare Earths*, edited by J. K. A. Gschneider and L. Eyring (North-Holland, Amsterdam, 1979), Vol. 2, p. 507.  
<sup>6</sup>J. S. Moodera, X. Hao, G. A. Gibson, and R. Meservey, *Phys. Rev. Lett.* **61**, 637 (1988).  
<sup>7</sup>F. Maccherozzi, M. Sperl, G. Panaccione, J. Minár, S. Polesya, H. Ebert, U. Wurstbauer, M. Hochstrasser, G. Rossi, G. Woltersdorf, W. Wegscheider, and C. H. Back, *Phys. Rev. Lett.* **101**, 267201 (2008).  
<sup>8</sup>E. Blackburn, C. Sanchez-Hanke, S. Roy, D. J. Smith, J.-I. Hong, K. T. Chan, A. E. Berkowitz, and S. K. Sinha, *Phys. Rev. B* **78**, 180408(R) (2008).  
<sup>9</sup>J. van Lierop, K.-W. Lin, J.-Y. Guo, H. Ouyang, and B. W. Southern, *Phys. Rev. B* **75**, 134409 (2007).  
<sup>10</sup>J. van Lierop, B. W. Southern, K.-W. Lin, Z.-Y. Guo, C. L. Harland, R. A. Rosenberg, and J. W. Freeland, *Phys. Rev. B* **76**, 224432 (2007).  
<sup>11</sup>C. Müller, H. Lippitz, J. J. Paggel, and P. Fumagalli, *J. Appl. Phys.* **99**, 073904 (2006).  
<sup>12</sup>P. Fumagalli, A. Schirmeisen, and R. J. Gambino, *Phys. Rev. B* **57**, 14294 (1998).  
<sup>13</sup>M. Taborelli, R. Allenspach, G. Boffa, and M. Landolt, *Phys. Rev. Lett.* **56**, 2869 (1986).  
<sup>14</sup>C. Müller, H. Lippitz, J. J. Paggel, and P. Fumagalli, *J. Appl. Phys.* **95**, 7172 (2004).  
<sup>15</sup>M. Szot, L. Kowalczyk, T. Story, V. Domukhovski, W. Knoff, K. Gas, V. V. Volobuev, A. Yu. Sipatov, and A. G. Fedorov, *Acta Phys. Pol. A* **114**, 1397 (2008).  
<sup>16</sup>U. Rücker, S. Demokritov, R. R. Arons, and P. Grünberg, *J. Magn. Magn. Mater.* **156**, 269 (1996).  
<sup>17</sup>J. Tang, C. E. O'Connor, and L. Feng, *J. Alloys Compd.* **275-277**, 606 (1998).  
<sup>18</sup>A. Stachow-Wójcik, T. Story, W. Dobrowolski, M. Arciszewska, R. R. Gałazka, M. W. Kreijveld, C. H. W. Swüste, H. J. M. Swagten, W. J. M. de Jonge, A. Twardowski, and A. Y. Sipatov, *Phys. Rev. B* **60**, 15220 (1999).  
<sup>19</sup>J. D. Hanawalt, H. W. Rinn, and L. K. Frevel, *Anal. Chem.* **10**, 471 (1938).  
<sup>20</sup>Swansom and Fuyat, *Natl. Bur. Stand. Circ. (U. S.)* **539**, 19 (1993).  
<sup>21</sup>H. Kepa, J. Kutner-Pielaszek, J. Blinowski, A. Twardowski, C. F.

- Majkrzak, T. Story, P. Kacman, R. R. Gałazka, K. Ha, H. J. M. Swagten, W. J. M. de Jonge, A. Y. Sipatov, V. Volobuev, and T. M. Giebultowicz, *Europhys. Lett.* **56**, 54 (2001).
- <sup>22</sup>U. Rücker, S. O. Demokritov, J. Nassar, and P. Grünberg, *Europhys. Lett.* **66**, 736 (2004).
- <sup>23</sup>W. H. Meiklejohn, *J. Appl. Phys.* **33**, 1328 (1962).
- <sup>24</sup>M. W. J. Chase, in *NIST Chemistry WebBook*, NIST Standard Reference Database No. 69 (National Institute of Standards and Technology, Gaithersburg, MD, 2009); <http://webbook.nist.gov>; *J. Phys. Chem. Ref. Data Monogr.* **9**, 1 (1998).
- <sup>25</sup>P. Balaz and E. Dutkovm, *Chem. Sust. Dekelop.* **15**, 127 (2007).
- <sup>26</sup>T. Takayama and H. Takagi, *Appl. Phys. Lett.* **88**, 012512 (2006).
- <sup>27</sup>J. L. Horwood, M. Townsend, and A. H. Webster, *J. Solid State Chem.* **17**, 35 (1976).
- <sup>28</sup>S. Couet, K. Schlage, R. Rüffer, S. Stankov, T. Diederich, B. Laenens, and R. Röhlberger, *Phys. Rev. Lett.* **103**, 097201 (2009).
- <sup>29</sup>J. Nogués and I. K. Schuller, *J. Magn. Magn. Mater.* **192**, 203 (1999).
- <sup>30</sup>P. Miltényi, M. Gierlings, M. Bammig, and U. May, *Appl. Phys. Lett.* **75**, 2304 (1999).
- <sup>31</sup>H. Ouyang, K.-W. Lin, C.-C. Liu, S.-C. Lo, Y.-M. Tzeng, J. Y. Guo, and J. van Lierop, *Phys. Rev. Lett.* **98**, 097204 (2007).
- <sup>32</sup>A. Paul, C. M. Schneider, and J. Stahn, *Phys. Rev. B* **76**, 184424 (2007).
- <sup>33</sup>J. Nogués, C. Leighton, and I. K. Schuller, *Phys. Rev. B* **61**, 1315 (2000).
- <sup>34</sup>J. Nogués, D. Lederman, T. J. Moran, and I. K. Schuller, *Phys. Rev. Lett.* **76**, 4624 (1996).
- <sup>35</sup>I. A. Campbell, *J. Phys. F: Met. Phys.* **2**, 47 (1972).